Veterinary Microbiology 230 (2019) 110–116

Contents lists available at ScienceDirect

Veterinary Microbiology

journal homepage: www.elsevier.com/locate/vetmic

Identification and evaluation of antivirals for Rift Valley fever virus

Yuekun Lang[a], Yonghai Li[a], Dane Jasperson[b], Jamie Henningson[a], Jinhwa Lee[a], Jingjiao Ma[a], Yuhao Li[a], Michael Duff[a], Haixia Liu[a], Dingping Bai[a], Scott McVey[b], Juergen A. Richt[a], Tetsuro Ikegami[c], William C. Wilson[b], Wenjun Ma[a,*]

[a] Department of Diagnostic Medicine/Pathobiology, Kansas State University, Manhattan, KS, USA
[b] USDA, ARS, Arthropod-Borne Animal Diseases Research Unit (ABADRU), Center for Grain and Animal Health Research, Manhattan, KS, USA
[c] Department of Pathology, The University of Texas Medical Branch at Galveston, Galveston, TX, USA

ARTICLE INFO

Keywords:
Rift Valley fever virus
MP-12 vaccine strain
Antiviral
Mitoxantrone
BSL-2 environment

ABSTRACT

Rift Valley fever virus (RVFV) is the causative agent of Rift Valley fever (RVF) that affects both livestock and humans. There are neither fully licensed RVF vaccines available for human or animal use, nor effective antiviral drugs approved for human use in the U.S. To identify antiviral compounds effective for RVF, we developed and employed a cell-based high-throughput assay using a recombinant RVFV MP-12 strain, which expresses Renilla luciferase in place of the NSs protein, to screen 727 small compounds purchased from the National Institutes of Health. Twenty-three compounds were initially identified using the screening assay. Two compounds, 6-azauridine and mitoxantrone, also inhibited the replication of the parental MP-12 strain encoding the NSs gene, with limited cytotoxic effects. The respective 50% inhibitory concentrations were 29.07 μM and 79.85 μM when tested with the parental MP-12 strain at a multiplicity of infection of 2. The compounds were further evaluated using the STAT-1 KO mouse model. At one hour post intranasal inoculation of MP-12 strain, mice were intranasally treated with each indicated compound twice daily. Mice treated with either placebo or 6-azauridine displayed severe weight loss and reached the threshold for euthanasia with obvious neurologic symptoms. Onset of disease was, however, delayed in mice treated with either ribavirin or mitoxantrone. The results indicated that mitoxantrone can reduce the severity of diseases in RVFV-infected mice. Our studies build the foundation for the initial screening and efficacy studies of RVF antivirals in a BSL-2 environment, avoiding the higher risks of BSL-3 exposure with wild-type virus.

1. Introduction

Rift Valley fever virus (RVFV) is the etiologic agent of Rift Valley fever (RVF) that affects both livestock and humans. RVFV is an arbovirus belonging to the genus *Phlebovirus* of the *Phenuiviridae* family, and was first identified during an investigation into an epidemic among sheep in the Rift Valley region of Kenya in 1930 (Daubney et al., 1931). Since then, countries in Africa have experienced numerous RVF outbreaks. In 2000, a severe RVF epidemic occurred outside of Africa in Yemen and Saudi Arabia that resulted in significant human morbidity and mortality (Balkhy and Memish, 2003; Shoemaker et al., 2002). In 2016, an imported human case of RVF was reported in China (Liu et al., 2017). The single infected patient had recently returned from a trip to Angola, Africa, where no active RVF outbreaks underwent during the period (Liu et al., 2017). In the last decade, the Centers for Disease Control and Prevention in the United States of America (U.S.) estimates the total mortality rate of hospitalized RVF patients to be approximately 10%. The trend towards global dissemination of RVF poses a significant threat to not only the livestock industry but also to public health (Ahmed et al., 2009; Liu et al., 2017).

Neither effective antiviral drugs nor commercial, fully licensed vaccines are available in the U.S. for human or animal use (Atkins and Freiberg, 2017; Reed et al., 2013). Phylogenetic data supports the conclusion that the genetic diversity of all characterized strains of RVFV remains relatively small (Bird et al., 2007; Grobbelaar et al., 2011; Ikegami, 2012). This limited genetic diversity suggests that antivirals effective for one strain should be active against all RVFV strains. The only conditionally licensed vaccine in the U.S. for animal use, MP-12, was derived from the pathogenic strain ZH548, which was attenuated after 12 serial passages in the presence of 5-fluorouracil in human diploid lung MRC-5 cells (Caplen et al., 1985; Ikegami et al., 2015). Mutations within the M and L segments play more critical roles in the

* Corresponding author.
E-mail address: wma@vet.k-state.edu (W. Ma).

https://doi.org/10.1016/j.vetmic.2019.01.027
Received 16 November 2018; Received in revised form 25 January 2019; Accepted 28 January 2019
0378-1135/

attenuation of the MP-12 compared to those mutations in the NSs gene (Ikegami et al., 2015). Due to significant attenuation, MP-12 strain is the Risk Group 2 virus, and exempted from the select agent regulations in the U.S.

To identify potential antiviral compounds, we developed a cell-based assay using the RVFV rMP12-rLuc strain, which encodes *Renilla* luciferase gene in place of NSs gene (Ikegami et al., 2006), and employed it to screen two NIH Clinical Collections including more than 700 compounds for antiviral activity. This initial screen was followed by confirmation of inhibitory effects using the rMP12-GFP strain, which encodes green fluorescent protein (GFP) gene in place of NSs gene, and further by the plaque reduction assay using the parental MP-12 strain. Cytotoxicity of the antiviral candidates was determined in different concentrations of compounds, and the 50% inhibitory concentrations (IC_{50}) were further determined by plaque reduction assay using the parental MP-12 strain.

Two candidates, 6-azauridine and mitoxantrone, were identified to efficiently inhibit the replication of the MP-12 strain. These two compounds had limited cytotoxic effects *in vitro* in Vero E6 cells. Both candidate compounds were further evaluated in STAT-1 KO mice in a BSL-2 environment using the ribavirin as a treatment control (Lang et al., 2016). Efficacy of these tested compounds was determined by comparisons of clinical signs, disease outcomes, virus replication and viremia, and histopathology.

2. Materials and methods

2.1. Ethics statements

All animal studies were approved and carried out in strict accordance to the recommendations of the guidelines of the Institutional Animal Care and Use Committee at Kansas State University, an AAALAC institution. Mouse studies were performed in a BSL-2 vivarium in the Comparative Medicine Group at Kansas State University facilities.

2.2. Cells, viruses, small molecule compounds and animals

African green monkey kidney epithelial (Vero) E6 cells (ATCC-CRL 1586) were maintained in the growth medium including 1x DMEM medium supplemented with 10% fetal bovine serum (FBS, Atlanta Biologicals). The RVFV MP-12 strain was kindly provided by the U.S. Army Medical Research Institute for Infectious Diseases. The RVFV rMP12-rLuc and rMP12-GFP strains were described previously (Ikegami et al., 2006). Propagations of the parental MP-12, recombinant rMP12-rLuc strain or rMP12-GFP strain were done by infecting confluent Vero E6 cells with a multiplicity of infection (MOI) of 0.01 of each virus in growth medium. Cell cultures were collected when approximately 70–80% of the infected cells showed cytopathic effects. The titer of viral stock was determined and calculated as 50% tissue culture infective dose per mL ($TCID_{50}$/mL) based on the presence of cytopathic effects. Two NIH Clinical Collections including total of 727 compounds were purchased from Evotec (South San Francisco, CA) and each compound was dissolved in the dimethyl sulfoxide (DMSO). Seven-week-old female STAT-1 KO mice were purchased from Taconic Biosciences (Hudson, NY).

2.3. Cell-based high-throughput screening assay

Time course analysis was performed first to determine the optimal infection dose and observation time. Briefly, 90% confluent Vero cells in a 96-well plate were infected with rMP12-rLuc in a triplicate at four different MOIs of 0.5, 1.0, 2.0, and 5.0. Cells were mock-infected with phosphate-buffered saline (PBS) to serve as the negative control. One hour post infection (hpi), cells were washed three times with PBS to remove the unattached virus. At 24, 36, 48, and 60 hpi, 20 µl supernatants of the infected cells in these 96-well plates were collected to test the luciferase signals using *Renilla* Luciferase Assay (Promega, Madison, WI) following the manufacturer's instructions. Luminescence quantification of each of the samples was immediately determined using a microplate reader (FLUOstar Omega, Cary, NC).

Z-factor analysis, which is an attempt to quantify the suitability of a particular assay for use in a full-scale high throughput screening assay, was utilized to determine the ideal time post infection and MOI for the high-throughput screening assay. The statically ideal Z-factor is 1.0. When the Z-factor value is between 0.5 and 1.0, the experiment can be considered as an excellent assay. When the Z-factor value is between 0 and 0.5, the experiment can be considered as a marginal assay. If the Z-factor value is less than 0, the experiment cannot be used in the high-throughput screening based on previous publications (Zhang et al., 1999; Zhang, 2008).

All tested compounds, postive control ribavirin and negative control were dissolved in DMSO, and were diluted in the growth medium for further assays. The 727 compounds were screened to identify potential RVFV inhibitors. All compounds were diluted in a final working concentration of 200 µM and the high-throughput screening was established in a 96-well format. Vero E6 cells were seeded in 96-well plates and infected with 2 MOI of the rMP12-rLuc virus. In order to identify the most effective antivirals, a low concentration of 20 µM of each compound was added to each well for initial screening at 1 hpi. Three wells were infected with the rMP12-rLuc virus following non-treatment (mock) or treatment with 20 µM ribavirin in the growth medium as the negative and positive controls, respectively. At 36 hpi, *Renilla* Luciferase Assay (Promega, Madison, WI) was performed as described above. The raw intensity data from each plate was normalized to the same Luminescence (RLU) scale. The average value of each compound from three independent experimental treatments was compared with that of the negative control. The compounds that significantly inhibited virus replication (the student *t*-test, $p \leq 0.05$) were selected for further analysis.

2.4. Inhibition efficacy and cytotoxicity tests

Vero E6 cells were seeded in 96-well plates and then infected with 2 MOI of the rMP12-GFP virus. Cells were infected without treatment as the non-treatment control. Cells that were infected with the rMP12-GFP virus and treated with 20 µM of ribavirin were the positive control. The 20 µM compounds selected from the high-throughput screening were added to the plate at 1 hpi. Cells were imaged at an 12-hour interval with Nikon Eclipse TE2000-S inverted phase microscope (Nikon, Melville, NY) using excitation/emission wavelength of 470/505 (GFP, green).

Cellular toxicity was assayed for each of selected 23 compounds with a final concentration of 40 µM using ToxiLight^{TM} bioassay kit (Lonza, Anaheim, CA) according to manufacturer's instructions. The plate was read by a microplate reader (FLUOstar Omega, Cary, NC).

2.5. Plaque reduction assay

Vero E6 cells with approximately 90% confluence in 6-well plates were infected with approximately 40 $TCID_{50}$ of the MP-12 virus in each well in the presence of each tested candidate at a final concentration of 40 µM in the growth medium. Cells infected with RVFV MP-12 without treatment were used as a negative control of plaque reduction assay. Cells treated with ribavirin at a final concentration of 40 µM were used as the positive control. Agar overlay was added at 1 hpi and the cells were incubated for 4 days at 37 ℃ followed by staining with 0.4% crystal violet. The compounds that reduced at least 50% plaques compared to the virus control were considered as effective antiviral candidates for further testing.

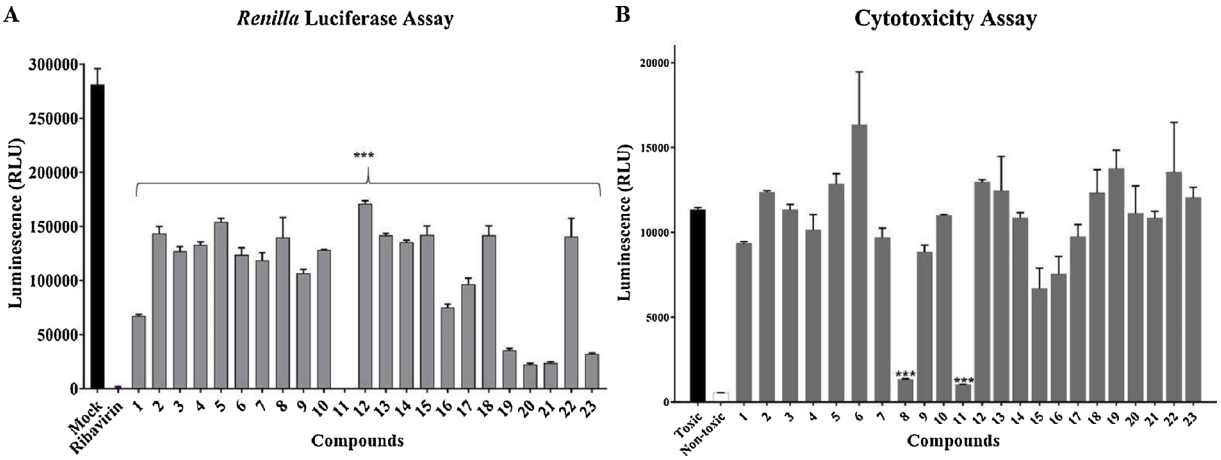

Fig. 1. Antiviral compound screening and cytotoxicity test.

A) Screening of antiviral compounds by a cell-based high-throughput assay using RVFV rMP12-rLuc strain. Cells were infected with rMP12-rLuc, and then treated with 20 μM each tested compound. Cells were only infected with rMP12-rLuc without treatment as the mock treatment, and cells were treated with ribavirin at 20 μM after infection as the positive control. A significant lower of luminescence was detected in the tested compounds 1 –23. The data are presented as the mean ± SEM of three independent experiments (*** $P < 0.001$).

B) Cytotoxicity test for each potential compound with indicated concentrations. ToxiLight 100% lysis reagent set (Lonza) was used as the toxic control, and the supernatant was collected from healthy Vero E6 cell culture as the non-toxic control. Vero E6 cells were treated with each compounds with 40 μM as indicated. Limited cytotoxicity was observed on cells treated with either Compound 8 (mitoxantrone) or Compound 11 (6-azauridine). The data are presented as the mean ± SEM of three independent experiments (*** $P < 0.001$).

2.6. Half maximal inhibitory concentration (IC_{50})

Vero cells in 96 well plates were infected with the MP-12 strain at 2 MOI in the presence of serially 2-fold diluted mitoxantrone, 6-azauridine or ribavirin starting at 1000 μM. After 4 hpi, cells were washed three times with fresh DMEM followed by adding 100 μL of growth medium per well. Supernatants were collected from cell cultures at 3 dpi. Virus titer was determined by an immunocytochemistry assay. Briefly, Vero cells were infected with 10-fold serially diluted viral supernatant and cultured for 4 days. After fixation with methanol for 10 min, cells were incubated with a mouse monoclonal antibody against the N protein of RVFV for 1 h. The cells were then treated with a goat anti-mouse IgG (H + L) secondary antibody, HRP (Invitrogen). $TCID_{50}$ were determined and IC_{50} were calculated using the regression analysis.

2.7. Mouse experiment

Fifty-six seven-week-old female STAT-1 KO mice were divided into four infected groups (13 mice/group) and one non-infected control group (4 mice). Mice in each infected group were intranasally inoculated with 1.58×10^6 $TCID_{50}$ of the parental MP-12 virus in a volume of 70 μl (35 μl per nostril) under anesthesia using 4% isoflurane as described previously (Lang et al., 2016). At 1 hpi, the mice were treated with each antiviral twice daily at an 8-hour interval for ten days under light anesthesia with isoflurane based on a former publication with slight modifications (Oestereich et al., 2014). The single dose concentrations for ribavirin (https://pubchem.ncbi.nlm.nih.gov/compound/ribavirin#section = Interactions), 6-azauridine (www.sciencedirect.com), mitoxantrone (https://www.caymanchem.com) were 100 mg/kg, 50 mg/kg, and 0.1 mg/kg, respectively. These dose concentrations were determined based on the available mouse LD_{50} concentrations of each compound. One group of infected mice were placebo-treated with 0.8% sodium chloride as the infection control. Mice were weighed and observed daily for clinical signs. On 3 and 6 dpi, three infected mice from each group and two blank control mice were euthanized and necropsied. The remaining seven mice of each infected group were kept until the end of experiment. Mice were euthanized if more than 20% of body weight was lost after virus inoculation or showed clinical signs of neurologic disease. During necropsy, samples including half of liver or brain and blood were aseptically collected from each mouse. One half of the liver or the brain from each mouse was stored at -80℃ for virus detection, and the remaining half of these tissues was fixed in 10% formalin for histopathologic and immunohistochemical (IHC) analysis as described in our previous publications (Lang et al., 2016; Liu et al., 2012). Virus detection was performed using a 10% tissue homogenate in PBS that was generated by homogenizing twice for 1 min in a Mini BeadBeater-8 (Biospec Products) as described previously (Lang et al., 2016). The serum was separated from blood specimens for further real-time RT-PCR analysis (Lang et al., 2016).

2.8. Statistical analysis

The student *t*-test was used to analyze differences between groups for data collected at a given time point. A $p \leq 0.05$ was considered statistically significant.

3. Results

3.1. Screening antiviral compounds by high-throughput screening assay

To determine the optimal virus dose and observation time for the high-throughput screening assay, we did a time course analysis by infecting Vero cells using different MOIs of rMP12-rLuc virus to determine the Z factor. Results showed that the peak Z-factor was 0.73 at 36 hpi with 2 MOI infection dose, although analysis of several combinations of infectious doses and assay times resulted in Z-factors that were greater than 0.5 but they were lower than 0.7. These data indicate that the Z-factor of 0.73 at 36 hpi with 2 MOI infection dose is optimal and the assay at these conditions is optimal for the high throughput screening (Zhang et al., 1999; Zhang, 2008). Two NIH Clinical Collections of 727 compounds were screened for their antiviral activities. We used ribavirin as the postive control, which efficiently inhibited rMP12-rLuc replication (Fig. 1A). At 20 μM dose, luminescence values of 23 of the compounds tested in the screening assay were significantly different from that of the mock-treatment control, whereas the other 704 compounds did not inhibit RVFV rMP12-rLuc replication (Fig. 1A).

3.2. Inhibition efficacy and cytotoxicity of tested compounds

We further tested the inhibition efficacy of the identified 23 compounds using the rMP12-GFP strain. Results showed that reduced GFP signals were observed in infected cells treated with the compounds including 8, 11, 12, 13, 16, 18, 19, 21, or 23 when compared to the untreated and infected rMP12- GFP cells. This result indicates that these compounds were able to inhibit rMP12-GFP replication. No GFP signal was detected in ribavirin-treated cells. Interestingly, the Compound 11 inhibited rMP12-GFP replication as effectively as the ribavirin, whereas others compounds were less effective in inhibiting replication.

We also evaluated their cytotoxicity of the selected 23 compounds. Most of these 23 compounds were toxic to Vero E6 cells at the concentration of 40 μM (Fig. 1B). Compared to the toxic (positive) and (negative) non-toxic controls, Compound 8 (mitoxantrone) and 11 (6-azauridine) were significantly less cytotoxic (Fig. 1B) and both compounds also inhibited the rMP12- GFP replication at 20 μM dose.

Plaque reduction assays were completed to confirm the inhibition efficacy of these two compounds at 40 μM in cells infected with the parental MP-12 strain. This concentration was used because these compound were not toxic at this concentration based on results of the cytotoxicity assays. Results showed that cells treated with either 6-azauridine or mitoxantrone reduced more than 50% plaques when compared to mock-treated control (Fig. 2A). Furthermore, the dose-escalation study showed that the 6-azauridine and mitoxantrone reduced virus replication by approximately 7 log PFU/ml of the MP12 virus at a concentration of 1000 μM (Fig. 2B). The IC_{50} of 6-azauridine and mitoxantrone were 29.07 μM and 79.85 μM, respectively. Compared to the IC_{50} of ribavirin (36.79 μM), the 6-azauridine inhibited the replication of the MP-12 virus more effectively.

3.3. Clinical signs, morbidity and mortality of mice treated with candidate antiviral compounds

There were no clinical signs in the negative control mice which were neither infected with the MP-12 virus nor treated with any candidate compounds, and they gained weight normally during the study. These mice were euthanized on 3 or 6 dpi. There was continual weight loss that began on 2 dpi until the end of experiment in all mice that received either placebo treatment or 6-azauridine treatment (Fig. 3A). Obvious clinical signs, including decreased activity, huddling, hunched posture and ruffled fur, were observed at 3 dpi. All mice in these two groups reached the 20% weight loss threshold or became moribund at 8 dpi (Fig. 3B). Noticeable weight loss was observed in mice treated with ribavirin at 3 dpi, but the mice gained weight until 5 dpi. Mice in the

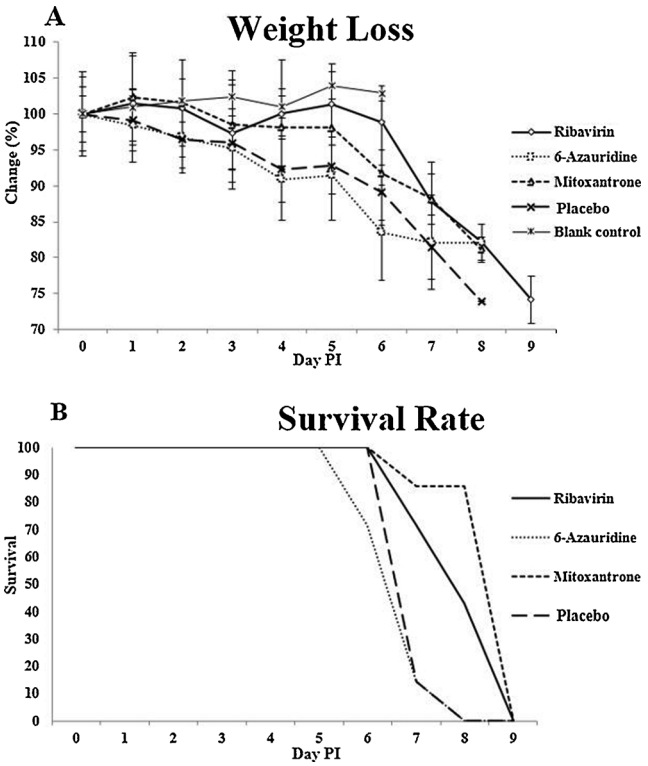

Fig. 3. Weight loss and survival rate of mice infected with the MP-12 and treated with different candidates. A): Weight loss of mice in different treatment groups (Mean ± SD); B): Survival rate of mice in different treatment groups. Mice in ribavirin and mitoxantrone treated groups survived one additional day than other two treatment groups, no significant difference was observed among groups.

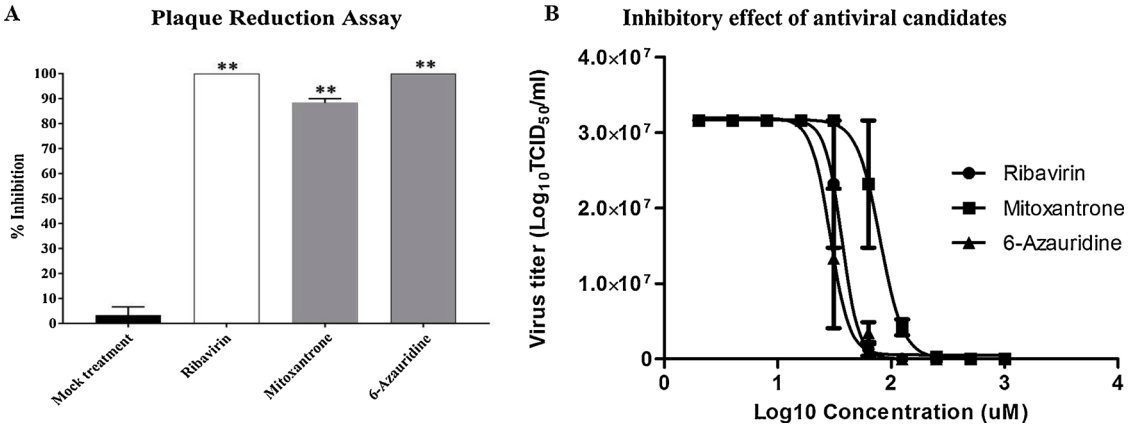

Fig. 2. *In vitro* charactization of identified antiviral compounds.
A) Plaque reduction of different compounds using the parental MP-12 strain.
Cells were only infected with the parental MP-12 without treatment as the mock control, and were treated with 40 μM of ribavirin after MP-12 infection as the positive control. Cells were treated with 40 μM of either mitoxantrone or 6-azauridine after MP-12 infection, the plaque numbers were counted. Plaque numbers in cells treated with either ribavirin or each tested compounds were significantly less than those on mock control cells only infected with the MP-12 strain. The data are presented as the mean ± SEM of three independent experiments (** $P < 0.01$).
B) *In vitro* antiviral activity of mitoxantrone and 6-azauridine.
The 50% inhibitory concentration of mitoxantrone, 6-azauridine and ribavirin on the parental MP-12 replication was determined on Vero cells. The cells were pretreated with serially 2-fold diluted mitoxantrone, 6-azauridine, or ribavirin for 4 h prior to infection, and were inoculated with MP12 at an MOI of 2. The virus infectious dose in the supernatants and a sigmoidal dose-response curve was fitted to the data using GraphPad Prism 6 (GraphPad Software).

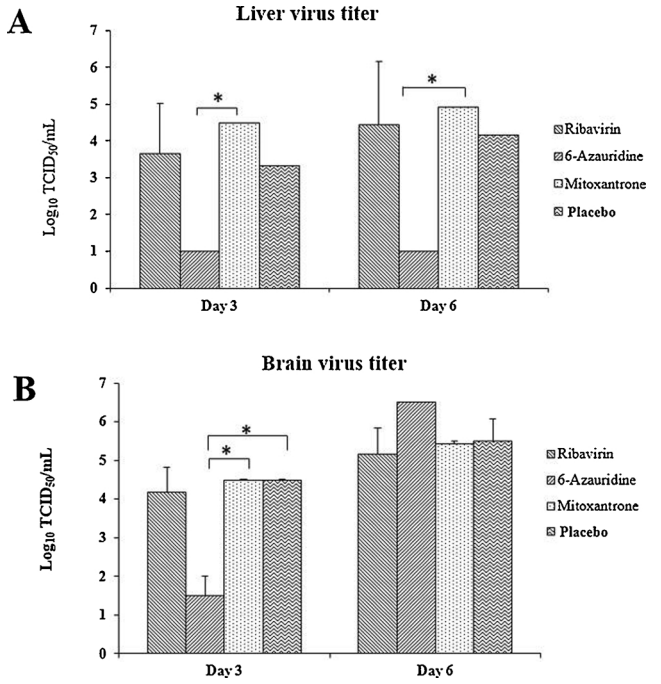

Fig. 4. Virus titers in mouse livers and brains collected on 3 and 6 dpi.
A): Virus titers in mouse livers. Virus was detected in the livers of mice from each groups on 3 and 6 dpi. A lower virus titer was observed in mouse livers of the 6-azauridine treatment group; B): Virus titers in mouse brains. Virus was detected in the brains of mice from all groups on 3 and 6 dpi. A significant lower virus titer was observed in mouse brains of the 6-azauridine treatment group on 3 dpi. The data are presented as the mean ± SEM (* $P < 0.05$).

mitoxantrone treated group lost weight beginning at 3 dpi, and less severe disease was observed overall when compared to placebo treated and to the 6-azauridine treated groups. However, there was dramatic weight loss after day 5 dpi in mitoxantrone treated mice. These observations were similar to the findings in the mice treated with the ribavirin (Fig. 3A). There was 100% mortality of all mice in each treatment group, although there was a one-day delay of mortality in both the ribavirin and mitoxantrone treated groups (Fig. 3B). No significant difference was observed in the survival rates between groups.

3.4. Viral replication and viremia in mice

Two negative control and three infected mice from each group were euthanized on 3 and 6 dpi, and viral titers in their livers and brains were determined. Virus was detected in liver specimens of mice from all infected groups on both days (Fig. 4A). The virus titers were lower in the liver specimens of 6-azauridine treated mice (10 $TCID_{50}$/mL) when compared to those of mice from the other infected groups. The virus titers detected in mice treated with the placebo, ribavirin, and with mitoxantrone were very similar (Fig. 4A). Clinical signs in mitoxantrone-treated group were less severe. Virus was recovered from the brains of each of the infected mice at both 3 and 6 dpi, indicating that all tested compounds did not block viral replication in brain tissues. However, a significantly lower titer was observed in the 6-azauridine-treated mice at 3 dpi, but not 6 dpi when compared to the placebo- or mitoxantrone-treated mice (Fig. 4B).

Real-time RT-PCR was performed to detect viral RNA in serum specimens prepared from blood collected from all mice. No viral RNA was detected in any of the specimens collected from ribavirin treated mice at any of the tested time points, similar to non-infected blank control mice (Table 1). In contrast, viral RNA was detectable in serum specimens from the other 3 treatment groups. Interestingly, mice treated with placebo were viremic only at 3 dpi, whereas viremia was

Table 1
RNA detection in mouse sera determined by a real-time RT-PCR assay.

	3 DPI	6 DPI	Humane euthanasia
Ribavirin	+ (0/3)*	+ (0/3)	+ (0/7)
6-Azauridine	+ (2/3)	+ (1/3)	+ (1/7)
Mitoxantrone	+ (3/3)	+ (1/3)	+ (1/7)
Placebo	+ (3/3)	+ (0/3)	+ (0/7)
Blank control	+ (0/2)	+ (0/2)	N/A

* RVFV RNA positive mouse numbers/ total mouse numbers.

detected at 3 and 6 dpi, or at the time of euthanasia, in sera collected from mice treated with either 6-azauridine or mitoxantrone.

3.5. Microscopic lesions and immunohistochemical detection of viral antigen

Liver and brain tissues collected from each mouse were examined for histopathological lesions and the presence of viral antigen, and the summarized histopathological scores are presented in Table 2. No lesions and no viral antigens were identified in brains and livers of negative control mice (Table 2, Fig. 5E and J). In livers, viral antigens were detected at both 3 and 6 dpi in each infected group. Sporadic extramedullary hematopoiesis was observed in 6-azauridine-treated group at 3 dpi and in ribavirin- or mitoxantrone-treated group at 6 dpi. No lesions were observed in livers collected from humanely euthanized mice of each treatment group. At 3 dpi, one out of three mice in the 6-azauridine-treated group had lesions in the brain, no lesions were identified in the brains of mice of the other groups. Only one out of three mice were antigen positive in the brains of the placebo-treated group at 3 dpi. Lesions in the brains were observed in all infected mice in each group at 6 dpi but the severity of the lesions were variable, and all humanely euthanized mice showed severe perivascular meningoencephalitis with necrosis (Table 2).

All mice euthanized at 6 dpi of the placebo treated group were encephalitic and the brain tissue lesions were characterized by necrosis with abundant necrotic cellular debris and meningitis. Abundant RVFV antigen was observed in the IHC (Fig. 5D and I). In ribavirin and 6-azauridine treated groups, the extent of necrosis and antigen labeling was apparently less and observed in only one out of three mice compared with the placebo-treated group at 6 dpi (Fig. 5A, C, F and H). In contrast, mice treated with mitoxantrone had moderate RVFV antigen presented in the neurons and the neuropil (Fig. 5B and G), and the disease was less severe than the placebo-treated group.

4. Discussion

RVFV has spread into non-endemic countries and is a significant threat to global public health and agriculture. There is an urgent need to develop effective antivirals for protecting exposed and infected humans. However, no effective antivirals have been approved for human RVF patients in the U.S. In this study, we developed a cell-based high throughput screening assay for inhibiting viral replication using the attenuated MP-12 strain expressing a reporter gene, and this assay was used to screen a total of 727 compounds. In the first round of screening using the recombinant MP-12 virus expressing luciferase, 23 compounds significantly reduced luminescence. This high hit rates could be false positive results due to multiple factors such as *i*) the interaction between the compound and the luciferin/luciferase, *ii*) compound toxicity and *iii*) cell viability or other factors. To confirm that these compounds indeed inhibit MP-12 replication, these 23 compounds were further tested using the recombinant MP-12 expressing GFP or the wild type MP12 using the plaque reduction assay. Two candidates including 6-azauridine and mitoxantrone were identified with efficient inhibition of MP-12 replication with low cytotoxicity at 20 or 40 μM doses, within the range of antiviral effect. These two compounds were further

Table 2
Histopathological (HE) and immunohistochemistry (IHC) scores for infected mice with different treatments.

	3 dpi				6 dpi			
	Liver		Brain		Liver		Brain	
	HE	IHC	HE	IHC	HE	IHC	HE	IHC
Ribavirin	0/3[a]	2/3 (1.0)	0/3	0/3	1/3 (2.0)	1/3 (1.0)	1/3 (2.0)	3/3 (2.0 ± 1.0)
6-Azauridine	1/3 (1.0)	3/3 (1.0)	0/3	0/3	0/3	2/3 (1.0)	1/3 (1.0)	3/3 (2.5 ± 0.5)
Mitoxantrone	0/3	3/3 (1.0)	0/3	0/3	1/3 (1.0)	1/3 (1.0)	3/3 (2.5 ± 0.5)	3/3 (3.0)
Placebo	0/3	3/3 (1.0)	0/3	1/3 (1.0)	0/3	2/3 (1.0)	3/3 (2.0 ± 1.0)	3/3 (2.5 ± 0.5)
Blank control	0/2	0/2	0/2	0/2	0/2	0/2	0/2	0/2

[a] Positive animals/total animals (mean histological score ± absolute deviation).

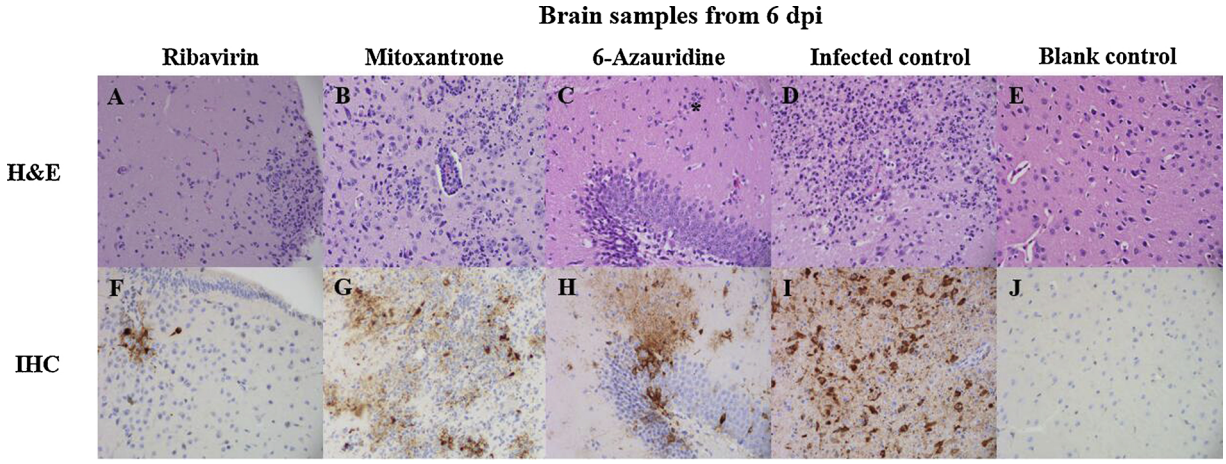

Fig. 5. H&E and IHC results from mouse brain samples collected at 6 dpi.
H&E results from different groups (A–E). A): In the ribavirin treated mice, there is a focal area of necrosis in the brain, the remainder of the brain section is normal. B): In the mitoxantrone treated mice, the brain has necrosis with necrotic cellular debris. C): In the 6-azauridine treated mice, there is a single small focal aggregate of inflammation (*) in the neuropil. D): In the non-infected and non-treated control mice, no lesions are observed and the brains are normal. E): In the infected control mice, the brain has extensive necrosis with abundant necrotic cellular debris.
IHC results from different groups (F–J). F): A focal area of RVFV antigen deposition is present in neurons and the neuropil in the ribavirin treated mouse brain. G): RVFV antigen is present in the neurons and the neuropil in mitoxantrone treated mouse brain. H): Moderate RVFV antigen is present in the neurons and the neuropil in the 6-azauridine treated mouse brain. I): No RVFV antigen was present in the non-infected and non-treated control mouse brain. J): Extensive RVFV antigen is present in the neurons and the neuropil in the infected control mouse brain. (H& E and IHC RVFV, ×400).

evaluated *in vivo* using the previously established mouse model in a BSL-2 environment (Lang et al., 2016). The therapeutic efficacy for effective antiviral drugs for RVFV infection likely depends on whether they are able to protect the central nervous system from lethal viral encephalitis (Bird and McElroy, 2016). We used the intransal route for treatment administration because intranasal delivery has been deomonstrated to be an alternative pratical method of delivery of small therapeutic molecules to the brain and spinal cord (Hanson and Frey, 2008). Using this route of administration, therapeutic agents were delivered to the brain via the olfatory and trigeminal pathways, therefore providing a direct connection with the CNS (Dixon et al., 2016; Ross et al., 2004; Thorne et al., 2004). All infected mice in this study were dead within 10 days, whereas we observed only a 50% mortality after infection with the MP-12 virus in our previous study (Lang et al., 2016). There are two reasons, which likely explain for this unexpected increase in mortality: *i*) the mice received significantly more stress in the present study, such as twice anesthesia daily, restraining for handling and weighing; *ii*) those mice may have been influenced by side effects from inhaled suspension treatment. Therefore, further optimization of the treatment administration (e.g., antiviral dosage, formulation, route, delivery device, frequency of anesthesia) should be considered for future studies (Vasa et al., 2015). In addition, inoculation of mice with RVFV through the intranasal route could be more virulent than the subcutaneous inoculation. This could also influence therapeutic outcomes. In a previous study, mice treated with ribavirin and challenged with RVFV via the subcutaneous route were partially protected, whereas treated mice exposed to RVFV by aerosol were not protected (Reed et al., 2013). This result suggests that early and aggressive RVFV invasion into CNS following aerosol exposure likely plays an important role in ribavirin's failure to prevent mortality among these animals (Reed et al., 2013). Therefore, RVFV inoculation routes (such as subcutaneous or intraperitoneal route) used for future animal studies to evaluate antiviral efficacy should be considered. Furthermore, although administration of the antiviral drugs via the intranasal route is expected to deliver to the brain, whether these antivirals were effectively delivered to the CNS needs further investigations. Especially, pharmacokinetics and pharmacodynamics of each of the candidates need to be determined in future studies.

Interestingly, viral RNA was detected in serum specimens of both 6-azauridine- and mitoxantrone-treated mice, but not detected in specimens collected from ribavirin-treated mice, indicating both newly identified compound candidates do not inhibit virmeia as effectively as the ribavirin does. Furthermore, neither of these two compounds nor the ribavirin did completely inhibit virus replicaiton as the virus was detected in both liver and brain tissues of infected mice in each treatment group. Mitoxantrone, however, delayed the progress of diseases in a similar manner to ribavirin, evidenced by the observation of clinical signs and mortality. Under these experimental conditions, however, there were no statistical differecnes in virus titers from the liver and brain tissues of mitoxantrone-treated mice when compared to other

treated groups. Mitoxantrone is an anthracenedione agent which inhibits Poxviruses replication by blocking virus assembly (Deng et al., 2007). In the presence of mitoxantrone, the protein precursors of vaccinia virus could be synthesized during virus infection, whereas there was limited post-translational processing of precursors to mature proteins (Deng et al., 2007). In addition, mitoxantrone is also likely to target a viral protein because mitoxantrone-resistant viruses could be generated and identified through virus passages in the presence of drug (Deng et al., 2007). However, mitoxantrone was reported to have little beneficial effect against vaccinia virus infection *in vivo* (Altmann et al., 2012; Deng et al., 2007). RVFV also synthesizes protein precursors (preglycoproteins) of Gn and Gc proteins during virus replication, yet it is not known whether the mitoxantrone employs a similar mechanism to limit RVFV replication. This possible mechanism of action needs to be investigated in future studies.

Noticeably, 6-azauridine could efficiently limit virus replication in livers of infected mice (both early and late time points), as well as in brains (early time point), compared to mitoxantrone or ribavirin, although no improved clinical outcomes were found in 6-azauridine treated mice. 6-azauridine is a synthetic triazine analogue of uridine with antimetabolite activity, which can inhibit multiplication of a broad range of DNA and RNA viruses (Crance et al., 2003; Neyts et al., 1996; Rada and Dragúň, 1977). However, the antiviral mechanism of 6-azauridine is still unknown. The reasons why the 6-azauridine efficiently inhibited RVFV replication but did not improve disease outcome need to be elucidated. The observation that the RVFV MP12 replicated rapidly from 3 to 6 dpi in 6-azauridine-treated mice may imply that a 6-azauridine-resistant virus strain emerged in the presence of this antiviral compound. The underlying mechanisms of 6-azauridine inhibition of RVFV replication and potential induction of resistant viruses should be investigated in future studies.

Taken together, two compounds - 6-azauridine and mitoxantrone - were identified by the cell-based high throughput screening and *in vitro* plaque reduction assays, and the subsequent therapeutic efficacy study in a mouse model demonstrated that the intranasal administration of mitoxantrone, but not 6-azauridine, has the potential to delay the disease progression after virus inoculation. Our studies build a foundation for further discovery and development of effective antivirals against RVFV infection.

Author disclosure statement

No competing financial interests exist.

Acknowledgements

We would like to thank the KSVDL Histopathology and Immunohistochemistry laboratory for the processing slides and Jennifer Phinney for helping the immunohistochemistry staining. This project was supported by Kansas State University Start-Up Fund (SRO# 001) and Grants of the Department of Homeland Security Center of Excellence for Emerging and Zoonotic Animal Diseases (CEEZAD), Grant no. 2010-ST061-AG0001, Agricultural Research Service and Kansas State NBAF Transition Funds.

References

Ahmed, J., Bouloy, M., Ergonul, O., Fooks, A., Paweska, J., Chevalier, V., Drosten, C., Moormann, R., Tordo, N., Vatansever, Z., Calistri, P., Estrada-Pena, A., Mirazimi, A., Unger, H., Yin, H., Seitzer, U., 2009. International network for capacity building for the control of emerging viral vector-borne zoonotic diseases: arbo-zoonet. Eurosurveillance 14, 11–14.

Altmann, S., Smith, A., Dyall, J., Johnson, R., Dodd, L., Jahrling, P., Paragas, J., Blaney, J., 2012. Inhibition of cowpox virus and monkeypox virus infection by mitoxantrone. Antiviral Res. 93, 305–308.

Atkins, C., Freiberg, A.N., 2017. Recent advances in the development of antiviral therapeutics for Rift Valley fever virus infection. Future Virol. 12, 651–665.

Balkhy, H., Memish, Z., 2003. Rift Valley fever: an uninvited zoonosis in the Arabian peninsula. Int. J. Antimicrob. Agents 21, 153–157.

Bird, B., McElroy, A., 2016. Rift Valley fever virus: unanswered questions. Antiviral Res. 132, 274–280.

Bird, B., Khristova, M., Rollin, P., Ksiazek, T., Nichol, S., 2007. Complete genome analysis of 33 ecologically and biologically diverse Rift Valley fever virus strains reveals widespread virus movement and low genetic diversity due to recent common ancestry. J. Virol. 81, 2805–2816.

Caplen, H., Peters, C., Bishop, D., 1985. Mutagen-directed attenuation of rift-valley fever virus as a method for vaccine development. J. Gen. Virol. 66, 2271–2277.

Crance, J., Scaramozzino, N., Jouan, A., Garin, D., 2003. Interferon, ribavirin, 6-azauridine and glycyrrhizin: antiviral compounds active against pathogenic flaviviruses. Antiviral Res. 58, 73–79.

Daubney, R., Hudson, J., Garnham, P., 1931. Enzootic hepatitis or Rift Valley fever. An undescribed virus disease of sheep cattle and man from East Africa. J. Pathol. Bacteriol. 34, 545–579.

Deng, L., Dai, P., Ciro, A., Smee, D., Djaballah, H., Shuman, S., 2007. Identification of novel antipoxviral agents: mitoxantrone inhibits vaccinia virus replication by blocking virion assembly. J. Virol. 81, 13392–13402.

Dixon, B., Chen, D., Zhang, Y., Flores, J., Malaguit, J., Nowrangi, D., Zhang, J., Tang, J., 2016. Intranasal administration of interferon Beta attenuates neuronal apoptosis via the JAK1/STAT3/BCL-2 pathway in a rat model of neonatal hypoxic-ischemic encephalopathy. ASN Neuro 8.

Grobbelaar, A., Weyer, J., Leman, P., Kemp, A., Paweska, J., Swanepoel, R., 2011. Molecular epidemiology of rift valley fever virus. Emerging Infect. Dis. 17, 2270–2276.

Hanson, L., Frey 2nd, W., 2008. Intranasal delivery bypasses the blood-brain barrier to target therapeutic agents to the central nervous system and treat neurodegenerative disease. BMC Neurosci. 9 (Suppl 3), S5.

Ikegami, T., 2012. Molecular biology and genetic diversity of Rift Valley fever virus. Antiviral Res. 95, 293–310.

Ikegami, T., Won, S., Peters, C., Makino, S., 2006. Rescue of infectious Rift Valley fever virus entirely from cDNA, analysis of virus lacking the NSs gene, and expression of a foreign gene. J. Virol. 80, 2933–2940.

Ikegami, T., Hill, T., Smith, J., Zhang, L., Juelich, T., Gong, B., Slack, O., Ly, H., Lokugamage, N., Freiberg, A., 2015. Rift valley fever virus MP-12 vaccine is fully attenuated by a combination of partial attenuations in the S, m, and l segments. J. Virol. 89, 7262–7276.

Lang, Y., Henningson, J., Jasperson, D., Li, Y., Lee, J., Ma, J., Li, Y., Cao, N., Liu, H., Wilson, W., Richt, J., Ruder, M., McVey, S., Ma, W., 2016. Mouse model for the Rift Valley fever virus MP12 strain infection. Vet. Microbiol. 195, 70–77.

Liu, Q., Qiao, C., Marjuki, H., Bawa, B., Ma, J., Guillossou, S., Webby, R.J., Richt, J.A., Ma, W., 2012. Combination of PB2 271A and SR polymorphism at positions 590/591 is critical for viral replication and virulence of swine influenza virus in cultured cells and in vivo. J. Virol. 86, 1233–1237.

Liu, J., Sun, Y., Shi, W., Tan, S., Pan, Y., Cui, S., Zhang, Q., Dou, X., Lv, Y., Li, X., Li, X., Chen, L., Quan, C., Wang, Q., Zhao, Y., Lv, Q., Hua, W., Zeng, H., Chen, Z., Xiong, H., Jiang, C., Pang, X., Zhang, F., Liang, M., Wu, G., Gao, G., Liu, W., Li, A., Wang, Q., 2017. The first imported case of Rift Valley fever in China reveals a genetic reassortment of different viral lineages. Emerg. Microbes Infect. 6, e4.

Neyts, J., Meerbach, A., McKenna, P., De Clercq, E., 1996. Use of the yellow fever virus vaccine strain 17D for the study of strategies for the treatment of yellow fever virus infections. Antiviral Res. 30, 125–132.

Oestereich, L., Rieger, T., Neumann, M., Bernreuther, C., Lehmann, M., Krasemann, S., Wurr, S., Emmerich, P., de Lamballerie, X., Olschlager, S., Gunther, S., 2014. Evaluation of antiviral efficacy of ribavirin, arbidol, and T-705 (favipiravir) in a mouse model for Crimean-Congo hemorrhagic fever. PLoS Negl. Trop. Dis. 8, e2804.

Rada, B., Dragúň, M., 1977. Antiviral action and selectivity of 6-Auridine. Ann. N. Y. Acad. Sci. 284, 410–417.

Reed, C., Lin, K., Wilhelmsen, C., Friedrich, B., Nalca, A., Keeney, A., Donnelly, G., Shamblin, J., Hensley, L., Olinger, G., Smith, D., 2013. Aerosol exposure to Rift Valley fever virus causes earlier and more severe neuropathology in the murine model, which has important implications for therapeutic development. PLoS Negl. Trop. Dis. 7, e2156.

Ross, T., Martinez, P., Renner, J., Thorne, R., Hanson, L., Frey 2nd, W., 2004. Intranasal administration of interferon beta bypasses the blood-brain barrier to target the central nervous system and cervical lymph nodes: a non-invasive treatment strategy for multiple sclerosis. J. Neuroimmunol. 151, 66–77.

Shoemaker, T., Boulianne, C., Vincent, M., Pezzanite, L., Al-Qahtani, M., Al-Mazrou, Y., Khan, A., Rollin, P., Swanepoel, R., Ksiazek, T., Nichol, S., 2002. Genetic analysis of viruses associated with emergence of Rift Valley fever in Saudi Arabia and Yemen, 2000-01. Emerging Infect. Dis. 8, 1415–1420.

Thorne, R., Pronk, G., Padmanabhan, V., Frey 2nd, W., 2004. Delivery of insulin-like growth factor-I to the rat brain and spinal cord along olfactory and trigeminal pathways following intranasal administration. Neuroscience 127, 481–496.

Vasa, D., O'Donnell, L., Wildfong, P., 2015. Influence of dosage form, formulation, and delivery device on olfactory deposition and clearance: enhancement of Nose-to-CNS uptake. J. Pharm. Innov. 10, 200–210.

Zhang, X., 2008. Novel analytic criteria and effective plate designs for quality control in genome-scale RNAi screens. J. Biomol. Screen. 13, 363–377.

Zhang, J., Chung, T., Oldenburg, K., 1999. A simple statistical parameter for use in evaluation and validation of high throughput screening assays. J. Biomol. Screen. 4, 67–73.